

World Journal of *Orthopedics*

World J Orthop 2023 September 18; 14(9): 662-732



MINIREVIEWS

- 662 Silver nanoparticle technology in orthopaedic infections
Jeyaraman M, Jeyaraman N, Nallakumarasamy A, Iyengar KP, Jain VK, Potty AG, Gupta A

ORIGINAL ARTICLE**Basic Study**

- 669 Formation process of extension knee joint contracture following external immobilization in rats
Zhou CX, Wang F, Zhou Y, Fang QZ, Zhang QB
- 682 Comparative study *in vivo* of the osseointegration of 3D-printed and plasma-coated titanium implants
Bondarenko S, Filipenko V, Ashukina N, Maltseva V, Ivanov G, Lazarenko I, Sereda D, Schwarzkopf R

Retrospective Study

- 690 Epidemiology of shoulder dislocations presenting to United States emergency departments: An updated ten-year study
Patrick CM, Snowden J, Eckhoff MD, Green CK, Scanaliato JP, Dunn JC, Parnes N
- 698 Sclerotherapy as a primary or salvage procedure for aneurysmal bone cysts: A single-center experience
Weber KS, Jensen CL, Petersen MM

Clinical Trials Study

- 707 Use of orthotics with orthotic sandals versus the sole use of orthotics for plantar fasciitis: Randomised controlled trial
Amoako-Tawiah P, Love H, Chacko Madathilethu J, LaCourse J, Fortune AE, Sims JMG, Ampat G

Observational Study

- 720 Relationships among body weight, lipids and bone mass in elderly individuals with fractures: A case-control study
Chen XX, Tian CW, Bai LY, Zhao YK, Zhang C, Shi L, Zhang YW, Xie WJ, Zhu HY, Chen H, Rui YF

ABOUT COVER

Editorial Board Member of *World Journal of Orthopedics*, Mohamed Sukeik, FRCS (Ed), MD, Chief Physician, Surgeon, Department of Trauma and Orthopaedics, Dr. Sulaiman Al-Habib Hospital-Al Khobar, Al Khobar 34423, Saudi Arabia. msukeik@hotmail.com

AIMS AND SCOPE

The primary aim of *World Journal of Orthopedics (WJO, World J Orthop)* is to provide scholars and readers from various fields of orthopedics with a platform to publish high-quality basic and clinical research articles and communicate their research findings online.

WJO mainly publishes articles reporting research results and findings obtained in the field of orthopedics and covering a wide range of topics including arthroscopy, bone trauma, bone tumors, hand and foot surgery, joint surgery, orthopedic trauma, osteoarthropathy, osteoporosis, pediatric orthopedics, spinal diseases, spine surgery, and sports medicine.

INDEXING/ABSTRACTING

WJO is now abstracted and indexed in PubMed, PubMed Central, Emerging Sources Citation Index (Web of Science), Scopus, Reference Citation Analysis, China Science and Technology Journal Database, and Superstar Journals Database. The 2023 Edition of Journal Citation Reports® cites the 2022 impact factor (IF) for *WJO* as 1.9. The *WJO*'s CiteScore for 2022 is 2.6.

RESPONSIBLE EDITORS FOR THIS ISSUE

Production Editor: Zi-Hang Xu, Production Department Director: Xiang Li, Editorial Office Director: Jin-Li Wang.

NAME OF JOURNAL

World Journal of Orthopedics

ISSN

ISSN 2218-5836 (online)

LAUNCH DATE

November 18, 2010

FREQUENCY

Monthly

EDITORS-IN-CHIEF

Massimiliano Leigheb, Xiao-Jian Ye

EXECUTIVE ASSOCIATE EDITORS-IN-CHIEF

Xin Gu

EDITORIAL BOARD MEMBERS

<http://www.wjgnet.com/2218-5836/editorialboard.htm>

PUBLICATION DATE

September 18, 2023

COPYRIGHT

© 2023 Baishideng Publishing Group Inc

PUBLISHING PARTNER

The Minimally Invasive Spine Surgery Research Center Of Shanghai Jiaotong University

INSTRUCTIONS TO AUTHORS

<https://www.wjgnet.com/bpg/gerinfo/204>

GUIDELINES FOR ETHICS DOCUMENTS

<https://www.wjgnet.com/bpg/GerInfo/287>

GUIDELINES FOR NON-NATIVE SPEAKERS OF ENGLISH

<https://www.wjgnet.com/bpg/gerinfo/240>

PUBLICATION ETHICS

<https://www.wjgnet.com/bpg/GerInfo/288>

PUBLICATION MISCONDUCT

<https://www.wjgnet.com/bpg/gerinfo/208>

POLICY OF CO-AUTHORS

<https://www.wjgnet.com/bpg/GerInfo/310>

ARTICLE PROCESSING CHARGE

<https://www.wjgnet.com/bpg/gerinfo/242>

STEPS FOR SUBMITTING MANUSCRIPTS

<https://www.wjgnet.com/bpg/GerInfo/239>

ONLINE SUBMISSION

<https://www.f6publishing.com>

PUBLISHING PARTNER'S OFFICIAL WEBSITE

https://www.shtrhospital.com/zkjs/info_29.aspx?itemid=647

Basic Study

Formation process of extension knee joint contracture following external immobilization in rats

Chen-Xu Zhou, Feng Wang, Yun Zhou, Qiao-Zhou Fang, Quan-Bing Zhang

Specialty type: Orthopedics**Provenance and peer review:**

Unsolicited article; Externally peer reviewed.

Peer-review model: Single blind**Peer-review report's scientific quality classification**

Grade A (Excellent): 0

Grade B (Very good): 0

Grade C (Good): C, C, C, C, C

Grade D (Fair): 0

Grade E (Poor): 0

P-Reviewer: Malkova TA, Russia; Nambi G, Saudi Arabia; Oommen AT, India**Received:** April 27, 2023**Peer-review started:** April 27, 2023**First decision:** June 14, 2023**Revised:** June 30, 2023**Accepted:** August 21, 2023**Article in press:** August 21, 2023**Published online:** September 18, 2023**Chen-Xu Zhou, Feng Wang, Yun Zhou, Quan-Bing Zhang**, Department of Rehabilitation Medicine, The Second Affiliated Hospital of Anhui Medical University, Hefei 230601, Anhui Province, China**Qiao-Zhou Fang**, The Second Clinical Medicine College, Anhui Medical University, Hefei 230000, Anhui Province, China**Corresponding author:** Yun Zhou, MD, PhD, Chief Physician, Professor, Department of Rehabilitation Medicine, The Second Affiliated Hospital of Anhui Medical University, No. 678 Fulong Road, Economic and Technological Development Zone, Hefei 230601, Anhui, China. zhouyunanhui@sina.com**Abstract****BACKGROUND**

Current research lacks a model of knee extension contracture in rats.

AIM

To elucidate the formation process of knee extension contracture.

METHODSWe developed a rat model using an aluminum external fixator. Sixty male Sprague-Dawley rats with mature bones were divided into the control group ($n = 6$) and groups that had the left knee immobilized with an aluminum external fixator for 1, 2, and 3 d, and 1, 2, 3, 4, 6, and 8 wk ($n = 6$ in each group). The passive extension range of motion, histology, and expression of fibrosis-related proteins were compared between the control group and the immobilization groups.**RESULTS**Myogenic contracture progressed very quickly during the initial 2 wk of immobilization. After 2 wk, the contracture gradually changed from myogenic to arthro-genic. The arthro-genic contracture progressed slowly during the 1st week, rapidly progressed until the 3rd week, and then showed a steady progression until the 4th week. Histological analyses confirmed that the anterior joint capsule of the extended fixed knee became increasingly thicker over time. Correspondingly, the level of transforming growth factor beta 1 (TGF- β 1) and phosphorylated mothers against decapentaplegic homolog 2 (p-Smad2) in the anterior joint capsule also increased with the immobilization time. Over time, the cross-sectional area of muscle fibers gradually decreased, while the amount of intermuscular collagen

and TGF- β 1, p-Smad2, and p-Smad3 was increased. Unexpectedly, the amount of intermuscular collagen and TGF- β 1, p-Smad2, and p-Smad3 was decreased during the late stage of immobilization (6-8 wk). The myogenic contracture was stabilized after 2 wk of immobilization, whereas the arthrogenic contracture was stabilized after 3 wk of immobilization and completely stable in 4 wk.

CONCLUSION

This rat model may be a useful tool to study the etiology of joint contracture and establish therapeutic approaches.

Key Words: Knee joint; Immobilization; Contracture; External fixator; Rats

©The Author(s) 2023. Published by Baishideng Publishing Group Inc. All rights reserved.

Core Tip: Current research lacks a model of knee extension contracture in rats. The study elucidated the formation process and therapeutic strategies of knee extension contracture. To this end, we developed a rat model using an aluminum external fixator. The results showed that the myogenic contracture was stabilized after 2 wk of immobilization, whereas the arthrogenic contracture was stabilized after 4 wk of immobilization. This rat model may be a useful tool to study the etiology of the joint contracture and establish therapeutic approaches.

Citation: Zhou CX, Wang F, Zhou Y, Fang QZ, Zhang QB. Formation process of extension knee joint contracture following external immobilization in rats. *World J Orthop* 2023; 14(9): 669-681

URL: <https://www.wjgnet.com/2218-5836/full/v14/i9/669.htm>

DOI: <https://dx.doi.org/10.5312/wjo.v14.i9.669>

INTRODUCTION

Knee contracture is currently one of the most common clinical diseases and is characterized by joint capsule fibrosis and a restricted range of motion (ROM) secondary to periarticular intermuscular connective tissue hyperplasia[1]. The signature pathology of joint contracture is the proliferation of myofibroblasts (active fibroblasts) and the deposition of proteins in the extracellular matrix in the joint capsule and intermuscular connective tissue[2]. The most common cause of knee contracture is prolonged immobilization, which is clinically used as an acute treatment for musculoskeletal disease to relieve knee pain and reduce inflammation[3,4]. Knee contracture is insidious and has adverse effects on function and quality of life, affecting daily activities such as ascending and descending stairs, walking, and toileting. Furthermore, knee contracture is very difficult to treat[5]. Despite a large amount of rehabilitation, conservative treatment, and even surgical treatment, it is difficult to completely restore the joint mobility, and this loss of mobility seriously decreases the quality of life of patients and adversely affects the distribution of medical resources in society[6,7]. It is therefore very important to investigate the mechanisms leading to knee contracture.

The contracture mechanism has been explored in many studies. As early as 1993, a rat flexion contracture model was successfully established by fixing the tibia and fibula in complete flexion (150) for up to 7 wk without damaging the joints [8]. In recent years, various immobilization methods have been introduced to create flexion contracture models by fixing the animal knee joint at about 150 of flexion, including hook buckle (a hook-and-loop fastener) immobilization and helix (spiral wire) immobilization[9,10]. By contrast, extension contracture models are rare. However, the extension contracture model is of clinical relevance because it better mimics fracture and bed-associated immobilization than the flexion contracture model.

According to the general international standard, the neutral position of the knee joint is the straightened or extended position, which is defined as 0. The functional position of the knee joint is from 15 to 20 of flexion, while the ROM of the normal knee is 120 to 150 for flexion and 5 to 10 for overextension. Knee injury usually requires immobilization in a straightened or functional position, but this type of immobilization may result in limited knee flexion motion (knee extension contracture); therefore, knee extension contracture is the most common type of knee contracture. Different fixation methods have different effects on muscles. If the muscle is fixed under the condition of being lengthened, its atrophy and the decrease of muscle contraction force will be less, and the ratio of fast and slow muscles of biceps femoris, which is often selected as the detection index of flexion knee contracture model, is also different from that of quadriceps femoris; however, the current literature describes several animal knee contracture models, most of which involve flexion knee contracture. The structure of the knee joint of rats is similar to that of humans and is easier to obtain compared to other animals. Thus, it is necessary to establish a convenient and reliable rat model of knee extension contracture.

In the present study, we studied the process of knee extension contracture formation during external fixation of the knee in a straightened position in a rat model that we developed. To the best of our knowledge, this is the first report of a rat model of knee extension contracture.

MATERIALS AND METHODS

A rat model of knee extension contracture

Male Sprague-Dawley (SD) rats (age 8 wk and weight 350 g +) were used in this experiment. Aluminum splints (6061; Longkai, Suzhou, China), sponge (33 d; Changzhou, China), and woodworking (BND-2815; Bonida, Guangdong, China) were prepared. The rats were kept under the same conditions without intervention for 2 wk before the experiment (free diet, day and night balance, temperature 20-25 °C, humidity 50% ± 5%). Each rat was placed on the operating table in the supine position and fixed. The fixing device and fixing schematic diagram is shown in [Figure 1](#). [Figure 2A](#) shows the results of applied fixation. [Figure 2B](#) shows the anterior X-ray of the rat knee joint, while [Figure 2C](#) shows the lateral X-ray of the rat knee joint. Immobilization was performed under general anesthesia achieved with an intraperitoneal injection of 10% chloral hydrate (0.03 mL/kg). A patent application has been made for the self-made aluminum splint (Patent No. ZL202120470158.0).

Measurements of the knee joints of 8-wk-old male rats ($n = 15$) revealed that the average thigh width was 3.23 cm ± 0.21 cm (range 6.38 ± 0.41 to 7.21 cm ± 0.43 cm) and the average calf width was 4.86 cm ± 0.27 cm (range 2.34 ± 0.13 to 5.11 cm ± 0.36 cm). In accordance with the anatomical characteristics of the rats, the immobilization device was shaped using a wire cutting process with an aluminum plate and bonded with a 0.5-cm-thick sponge on the skin to prevent excessive immobilization. The shape of the aluminum plate is shown in [Figure 1](#). The fixation device placed the knee joint in the straightened position and ensured complete external immobilization of the knee joint. The animal experiments described in this study were authorized by the Experimental Animal Ethics Committee of Anhui Medical University (No. LLSC20221126).

Grouping and specimen collection

Sixty rats were randomly divided into 10 groups ($n = 6$ in each group). The control group did not do any intervention, while the immobilization groups had the left hindlimb fixed for 1 d (immobilization-1 d group), 2 d (immobilization-2 d group), 3 d (immobilization-3 d group), 1 wk (immobilization-1 wk group), 2 wk (immobilization-2 wk group), 3 wk (immobilization-3 wk group), 4 wk (immobilization-4 wk group), 6 wk (immobilization-6 wk group), and 8 wk (immobilization-8 wk group). All groups were reared in the same environment, and the ROM of the knee joint was measured on the same day as the 8-wk-fixed group after controlling the fixed time. The rats in the appropriate group were euthanized by an excessive intraperitoneal injection of 10% chloral hydrate. After euthanasia, the fixed left hindlimb of the rat was removed at the hip joint. The skin was separated, and the knee mobility was measured using the measurement device designed for this experiment ([Figure 3](#)). Then the muscles were separated. The rectus femoris was divided into two parts: one part was frozen at -80 °C for protein molecular weight detection, while the other part was fixed in 4% paraformaldehyde for Sirius red staining. Knee mobility was measured after the separation of the muscles. The anterior joint capsule was divided into two parts: one part was frozen at -80 °C for protein molecular weight detection, while the other part was fixed in 4% paraformaldehyde for hematoxylin and eosin (H&E) staining. During the experiment, the rats were free to move within the cage with the immobilization device attached.

Measurement of joint mobility

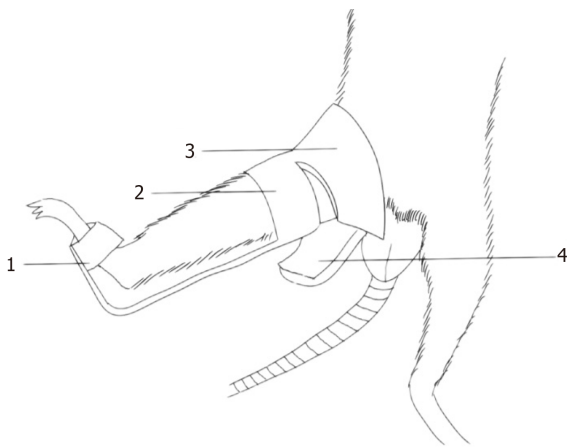
A joint mobility meter was used to measure the joint motion of the left knee of 60 SD rats ([Figure 3](#)). The Kirschner wire was penetrated from the femoral neck parallel to the femur. Fixed the cruzi needle by magnetic suction removable metal clamp. The distal tibia was secured to the turntable with disposable plastic ties. The digital force gauge was secured to the slide. On the base of the equipment was a rope attached to the groove of the turntable and a digital dynamometer. The turntable moved when the drive wheel was turned to indirectly turn the tibia while the femur was stationary. The applied force was displayed on the screen of the digital force meter, and the angular change between the femur and tibia (the disk radius, the force arm) was constant and was calculated according to the scale of the turntable. Therefore, the force moment and the force size showed a linear relationship. The moment size and the angle also had a corresponding relationship. The applied torque was calculated by multiplying the force by the constant radius of the disk. Knee ROM was measured with 5.3 N-cm as the standard torque. This torque brings the knee close to its physiological limit but does not damage the soft tissue[11-13]. The mobility of each left knee was measured three times by two researchers, giving six measurements. The knee ROM before and after myotomy was measured to yield the total, myogenic, and arthrogenic contracture using a previously described method[14]. (1) Degree of total contracture = ROM before myotomy (knee joint in the control group)-ROM before myotomy (knee joint in the immobilization group); (2) degree of arthrogenic contracture = ROM after myotomy (knee joint in the control group)-ROM after myotomy (knee joint in the immobilization group); and (3) degree of myogenic contracture = degree of total contracture-degree of arthrogenic contracture. A patent application has been made for the self-made joint mobility meter (Patent No. ZL202120996643.1).

Histological evaluation

Specimens used for joint mobility assessment were used to evaluate the histology of the knee joint. After the ROM measurements, the left rectus femoris and anterior knee joint capsule were fixed in 4% paraformaldehyde (pH 7.4) at 4 °C for approximately 36 h. The specimens were embedded in paraffin. The rectus femoris specimens were cut into 5-µm coronal sections, while the joint capsule specimens were sectioned into 5-µm sagittal sections.

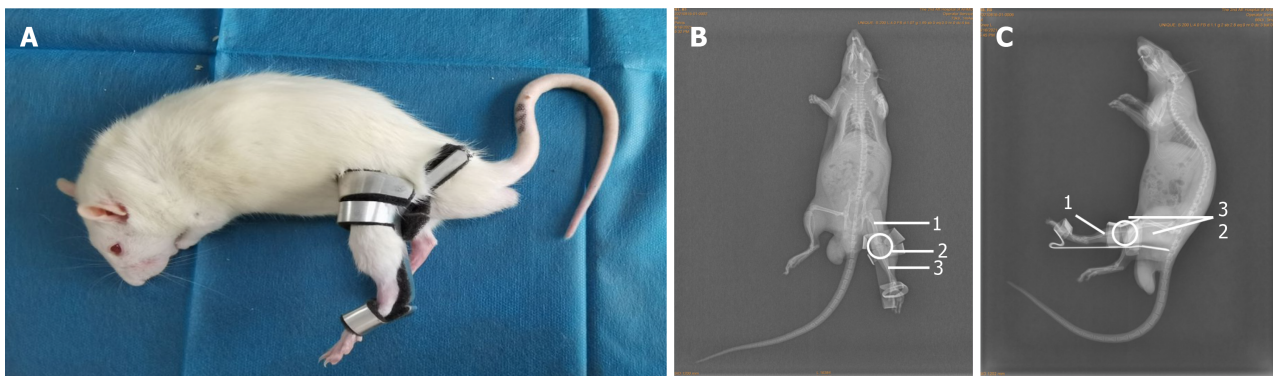
Sirius red staining

Rectus femoris sections were stained with Sirius red solution for 1 h (2610-10-8; Solarbio Life Science, Beijing, China) and rinsed with running water to remove the surface dye. Nuclei were stained with Mayer's hematoxylin solution for 8 to 10



DOI: 10.5312/wjo.v14.i9.669 Copyright ©The Author(s) 2023.

Figure 1 Knee joint fixation device. Immobilize the back of the rat's distal foot to prevent the rat's lower limb from slipping out of the immobilization device. Immobilize the periphery of the rat knee joint. Above the knee joint of the rat is an inverted conical structure, and this design fixes the periphery of the femur of the rat. Appropriate bending under the rat femur provides a lever fulcrum action. (1) Immobilize the back of the rat's distal foot to prevent the rat's lower limb from slipping out of the immobilization device. (2) Immobilize the periphery of the rat knee joint. (3) Above the knee joint of the rat is an inverted conical structure, and this design fixes the periphery of the femur of the rat. (4) Appropriate bending under the rat femur provides a lever fulcrum action.



DOI: 10.5312/wjo.v14.i9.669 Copyright ©The Author(s) 2023.

Figure 2 Fixed schematic diagram. A: Fixed picture; B: X-ray orthotopic slice of rat knee joint after immobilization; C: X-line lateral tablet of rat knee joint after immobilization. ¹Femur; ²Knee; ³Tibia.

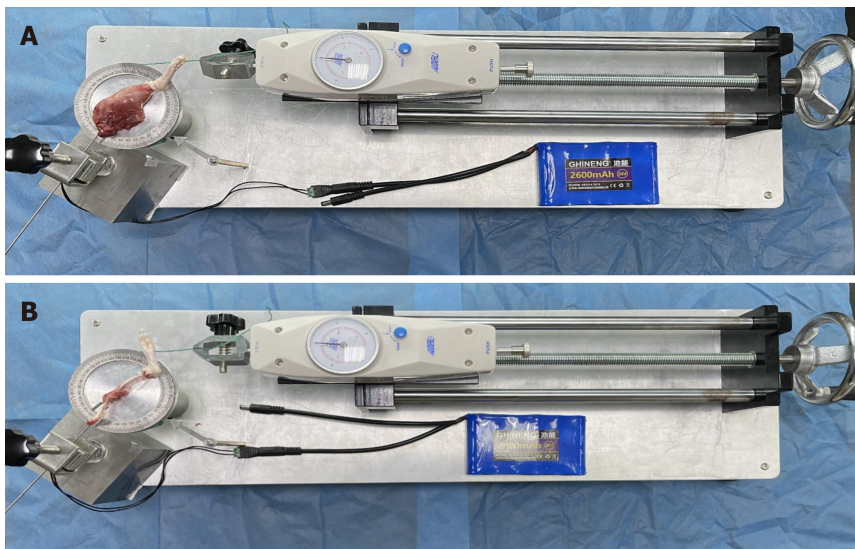
min and flushed with running water for 10 min. Sections were then conventionally dehydrated and sealed with neutral gum. The muscle collagen fiber density and muscle fiber cross-sectional area for each region were assessed using ImageJ software version 1.53a (National Institutes of Health, Bethesda, MD, United States, available at <https://imagej.nih.gov/ij/>). Histological analysis was performed on six rats in each group, with three slides for each rat.

H&E staining

The joint capsule sections were stained with H&E using the following steps. (1) Paraffin sections were dewaxed and then placed in xylene I for 10 min, xylene for 10 min, anhydrous ethanol I for 5 min, anhydrous ethanol for 5 min, 95% alcohol for 5 min, 90% alcohol for 5 min, 80% alcohol for 5 min, 70% alcohol for 5 min, and finally washed with distilled water; (2) Sections were stained with harris hematoxylin for 3-8 min, rinsed with tap water and differentiated with 1% ethanol hydrochloride for several seconds, and then rinsed with tap water again. The sections were returned to blue with 0.6% ammonia and rinsed with running water; (3) Sections were stained in eosin solution for 1-3 min; (4) To attain the dehydration seal, the sections were placed in 95% alcohol I for 5 min, 95% alcohol II for 5 min, anhydrous ethanol I for 5 min, anhydrous ethanol II for 5 min, xylene I for 5 min, and xylene II for 5 min; the sections were then removed from the xylene to dry and were sealed with neutral gum; and (5) Microscopic examination, image acquisition, and histological analysis were performed on six rats in each group, with three slides for each rat.

Immunohistochemistry

The following steps were used to prepare the articular capsule sections by immunohistochemistry. (1) Paraffin sections were dewaxed in the same way as H&E staining; (2) The 3% hydrogen peroxide was dropped onto the slice tissue, incubated at room temperature for 15 min, and washed with phosphate-buffered saline (PBS) for 3 times, 3 min each time; (3) After wiping the slide dry, the diluted normal goat serum was added and the slide was sealed at room temperature for



DOI: 10.5312/wjo.v14.i9.669 Copyright ©The Author(s) 2023.

Figure 3 Joint mobility meter. A: Peeling range of motion (total contracture) measurement; B: Measuring range of motion after muscle separation (arthrogenic contracture).

30 min; (4) The first antibody was added and incubated in a wet box at 4 °C overnight (15 h); (5) After PBS washing, the sections were dried with absorbent paper, and streptavidin-horseradish peroxidase conjugate labeled goat anti rabbit/mouse secondary antibody was added and incubated at 37 °C for 30 min; (6) After PBS washing, the PBS solution was removed and 3,3'-diaminobenzidine color developing solution was freshly prepared and added to each slice; (7) Mayer's hematoxylin re-staining was performed; and (8) Finally, dehydration and sealing, microscopic examination, image collection and histological analyses were performed the same way as H&E staining.

Proteomics analysis of muscle and joint capsule

Protein immunoblotting (western blotting) was performed as follows. Total protein was extracted from the retained muscle and joint capsule samples. When 50-60 mg rectus femoris muscle was taken, the total tissue protein was extracted with 600 mL radio immunoprecipitation assay (RIPA) reagent (Tris-HCl [pH 7.4], 150 mmol/L NaCl, 1 mmol/L ethyleneamineetraacetic acid, 1% Triton X-100, 1% sodium deoxycholate, 0.1% sodium dodecyl sulfate [SDS], and 1 mmol/L PMSF), and a protease inhibitor was added to the RIPA. Total proteins were separated by SDS-polyacrylamide gel electrophoresis and transferred to the polyvinylidene difluoride (PVDF) membrane. The PVDF was washed and immersed in 5% skim milk for 4 °C overnight. Membranes were incubated with anti-rat monoclonal antibody (1:10000-50000, cell signaling, United States) for 2 h at room temperature, and then washed three times with a Tris-buffered saline with 0.1% Tween 20 (TBST) solution (10 min/wash). The washed PVDF membrane was incubated with horseradish peroxidase-labeled goat anti-rat immunoglobulin G antibody (1: 10000-50000; Cell Signaling, Danvers, MA, United States) for 1 to 2 h at room temperature, washed with TBST (as described above), and then detected with enhanced chemiluminescence light-emitting liquid colored with energy autoexposure. The developing bands were analyzed by IPP software.

Statistical analysis

The results are expressed as the mean \pm standard deviation. One-way analysis of variance was used to test the difference between groups. $P < 0.05$ was statistically significant. Statistical analyses were performed using IBM SPSS statistics software, version 22 (IBM Corp., Armonk, NY, United States).

RESULTS

Three rats in the immobilization-6 wk group experienced slippage of the immobilization device in the 2nd week of immobilization; the immobilization device was fixed the same day as the slippage occurred, and there was no further slippage until the end of the immobilization period. There was no death, lower limb necrosis, or other complications in any group.

Total contracture, myogenic contracture, and arthrogenic contracture

After 1 wk of immobilization, the degree of total contracture significantly differed between the control group and the immobilization groups (all $P < 0.05$). Compared with the immobilization-1 d, -2 d, and -3 d groups, the degree of total contracture was significantly greater in the immobilization-1 wk, -2 wk, -3 wk, -4 wk, -6 wk, and -8 wk groups (all $P < 0.05$). Total contracture degree was not significantly different between certain adjacent immobilization groups, *i.e.* between the immobilization-1 d and -2 d, immobilization-2 d and -3 d, immobilization-3 wk and -4 wk, immobilization-4

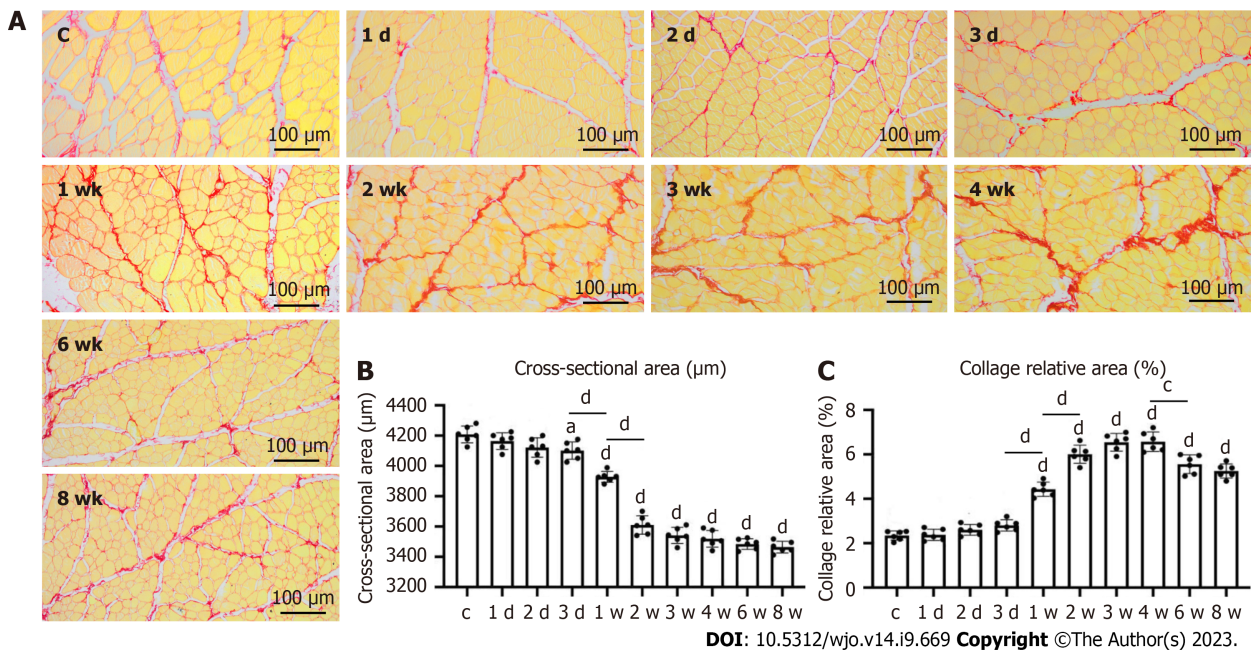


Figure 4 Sirius red staining findings. A: Morphological changes of rectus femoris after Sirius red staining, group C (control), 1 d, 2 d, 1 wk, 2 wk, 3 wk, 4 wk, 6 wk, and 8 wk; B and C: Cross-sectional value of rectus femoris fibers. * $P < 0.05$; ^a $P < 0.001$; ^b $P < 0.0001$.

wk and -6 wk, and immobilization-6 wk and -8 wk groups. The degree of total contracture was increased with the immobilization time (Table 1).

The degree of myogenic contracture was significantly greater in the immobilization-1 wk group than the immobilization-3 d group ($P < 0.05$). The degree of myogenic contracture also significantly differed between the immobilization-1 wk and -2 wk groups ($P < 0.05$), but not between any other adjacent immobilization groups ($P > 0.05$). The results suggested that myogenic contracture occurred after 1 wk of immobilization and gradually stabilized after 2 wk of immobilization, whereas the subsequent joint contractures were mostly arthrogenic (Table 1).

After 1 wk of immobilization, the degree of arthrogenic contracture was significantly greater in the immobilization groups than the control group ($P < 0.05$). The degree of arthrogenic contracture significantly differed between the immobilization-3 d and -1 wk, immobilization-1 wk and -2 wk, and immobilization-2 wk and -3 wk groups (all $P < 0.05$), but not between the other adjacent groups ($P > 0.05$). The results suggested that arthrogenic contracture progressed from 1 to 3 wk of immobilization. However, the progression amplitude of the arthrogenic contracture began to weaken after 3 wk of immobilization, after 4 wk, the arthrogenic contracture is basically stable (Table 1).

Histological evaluation of the Sirius red-stained sections

Compared with the control group, the mean diameter of the rectus femoris was significantly decreased with the duration of immobilization in all immobilization groups except the immobilization-1 d and -2 d groups ($P < 0.05$). From 1 d to 3 wk of immobilization, the proportion of collagen fibers in the rectus femoris of the immobilization groups increased with the fixation time. The proportion of collagen fibers significantly differed between the control group and all immobilization groups except the immobilization-1 d, -2 d, and -3 d groups ($P < 0.05$). The proportion of collagen fibers in the rectus femoris stabilized in the immobilization-4 wk group, but was decreased in the immobilization-6 wk and -8 wk groups ($P < 0.05$ in all cases; Figure 4).

Evaluation of the hematoxylin-eosin-stained sections and immunohistochemistry

The largest synovial area in the sagittal plane was analyzed. H&E staining showed that the degree of synovial hyperplasia of the anterior joint capsule in the immobilization groups increased with the fixation time, with significant differences between adjacent groups, *i.e.* between the immobilization-1 d and -2 d, immobilization-3 d and -1 wk, immobilization-1 wk and -2 wk, and immobilization-2 wk and -3 wk groups ($P < 0.05$). The degree of synovial hyperplasia of the anterior joint capsule also significantly differed between the control group and all immobilization groups, except the immobilization-1 d group ($P < 0.05$; Figure 5). Immunohistochemistry showed that the change trend of phosphorylated mothers against decapentaplegic homolog (p-Smad2) was consistent with the degree of synovial hyperplasia of the anterior joint capsule, but the percentage of p-Smad2 in each group was significantly different from that in the control group immobilization-2 d ($P < 0.05$; Figure 6).

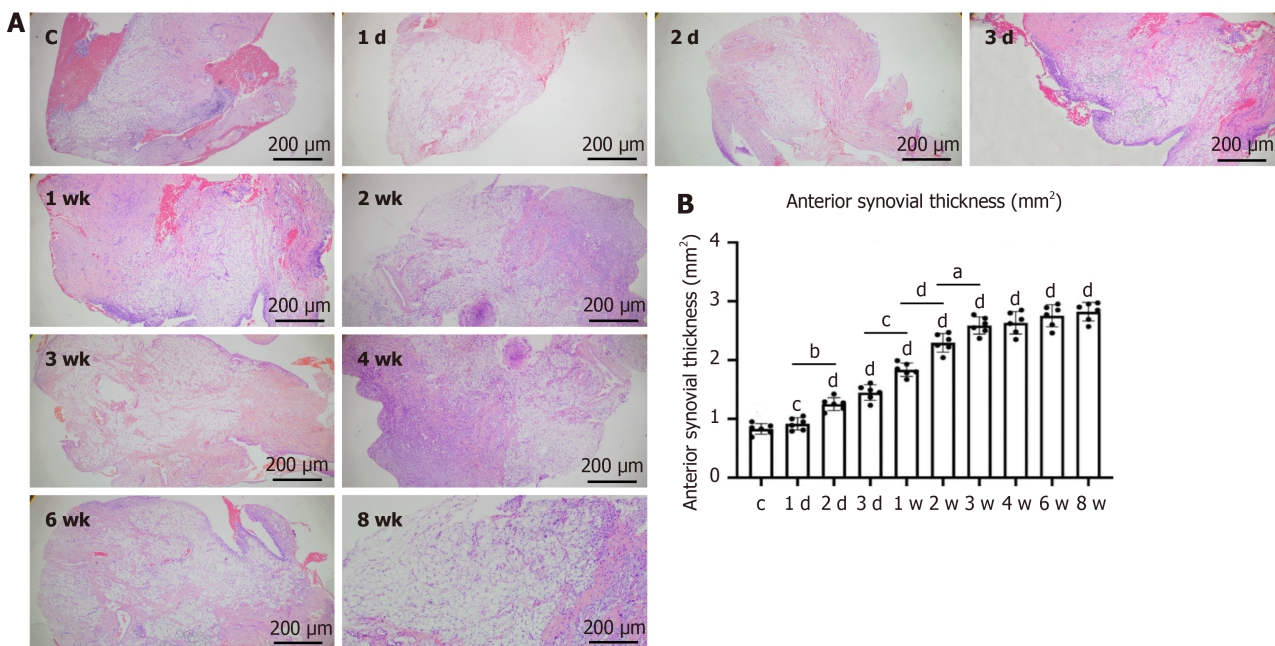
Protein expression in the muscle and joint capsule

After early joint immobilization, the expression level of transforming growth factor beta 1 (TGF-β1) was significantly increased in the joint capsule and muscles. The expression level of TGF-β1 in the joint capsule was significantly higher in the immobilization-1 wk group than in the immobilization-3 d group. TGF-β1 expression of joint capsule continued to

Table 1 Total, myogenic, and arthrogenic contracture after knee immobilization for various time periods in 60 SD rats (mean ± SD)

Grouping	Quantity	Degree of contracture		
		Total contracture	Myogenic contracture	Arthrogenic contracture
Control	6	0.0 ± 0.0	0.0 ± 0.0	0.0 ± 0.0
Immobilization-1 d	6	1.1 ± 0.6	0.6 ± 0.4	0.5 ± 0.3
Immobilization-2 d	6	2.4 ± 0.7	1.5 ± 0.4	0.9 ± 0.2
Immobilization-3 d	6	5.9 ± 1.0	4.0 ± 1.0	1.9 ± 0.5
Immobilization-1 wk	6	23.5 ± 2.0 ^{a,b,c,d}	15.9 ± 1.9 ^{a,b,c,d}	7.6 ± 0.7 ^{a,b,c,d}
Immobilization-2 wk	6	51.8 ± 1.8 ^{a,b,c,d,e}	32.7 ± 1.1 ^{a,b,c,d,e}	19.1 ± 1.3 ^{a,b,c,d,e}
Immobilization-3 wk	6	78.7 ± 2.2 ^{a,b,c,d,e,f}	33.9 ± 2.1 ^{a,b,c,d,e}	44.5 ± 1.9 ^{a,b,c,d,e,f}
Immobilization-4 wk	6	79.9 ± 2.8 ^{a,b,c,d,e,f}	34.2 ± 2.2 ^{a,b,c,d,e}	44.9 ± 2.2 ^{a,b,c,d,e,f}
Immobilization-6 wk	6	80.8 ± 3.5 ^{a,b,c,d,e,f}	35.5 ± 2.9 ^{a,b,c,d,e}	45.3 ± 2.9 ^{a,b,c,d,e,f}
Immobilization-8 wk	6	82.5 ± 3.0 ^{a,b,c,d,e,f}	35.9 ± 2.5 ^{a,b,c,d,e}	46.6 ± 2.3 ^{a,b,c,d,e,f}

^a*P* < 0.05 vs control group.
^b*P* < 0.05 vs immobilization-1 d group.
^c*P* < 0.05 vs immobilization-2 d group.
^d*P* < 0.05 vs immobilization-3 d group.
^e*P* < 0.05 vs immobilization-1 wk group.
^f*P* < 0.05 vs immobilization-2 wk group.



DOI: 10.5312/wjo.v14.i9.669 Copyright ©The Author(s) 2023.

Figure 5 Hematoxylin and eosin staining findings. A: Morphological changes of the anterior joint capsule; B: The anterior joint capsule thickness value. ^a*P* < 0.05; ^b*P* < 0.01; ^c*P* < 0.001; ^d*P* < 0.0001.

increase after immobilization for up to 8 wk. There were significant differences in TGF-β1 levels in the joint capsule between the immobilization-2 d and -3 d, immobilization-1 wk and -2 wk, and immobilization-2 wk and -3 wk groups (*P* < 0.05). The TGF-β1 content of the anterior joint capsule increased with the immobilization time, with a slight downward trend in the immobilization-8w group that did not reach statistical significance (*P* > 0.05). TGF-β1 expression in the anterior joint capsule was significantly increased in the control group compared with the immobilization groups (*P* < 0.05), except the immobilization-1 d and -2 d groups. Western blot analysis showed that the TGF-β1 content in the quadriceps muscle first increased and then decreased. The TGF-β1 content in the muscle significantly differed between the immobilization-2 d and -3 d, immobilization-3 d and -1 wk, immobilization-1 wk and -2 wk, and immobilization-6 wk and -8 wk groups (*P* < 0.05); The contents of Smad2 and Smad3 and TGF-β1 in quadriceps femoris had the same trend of

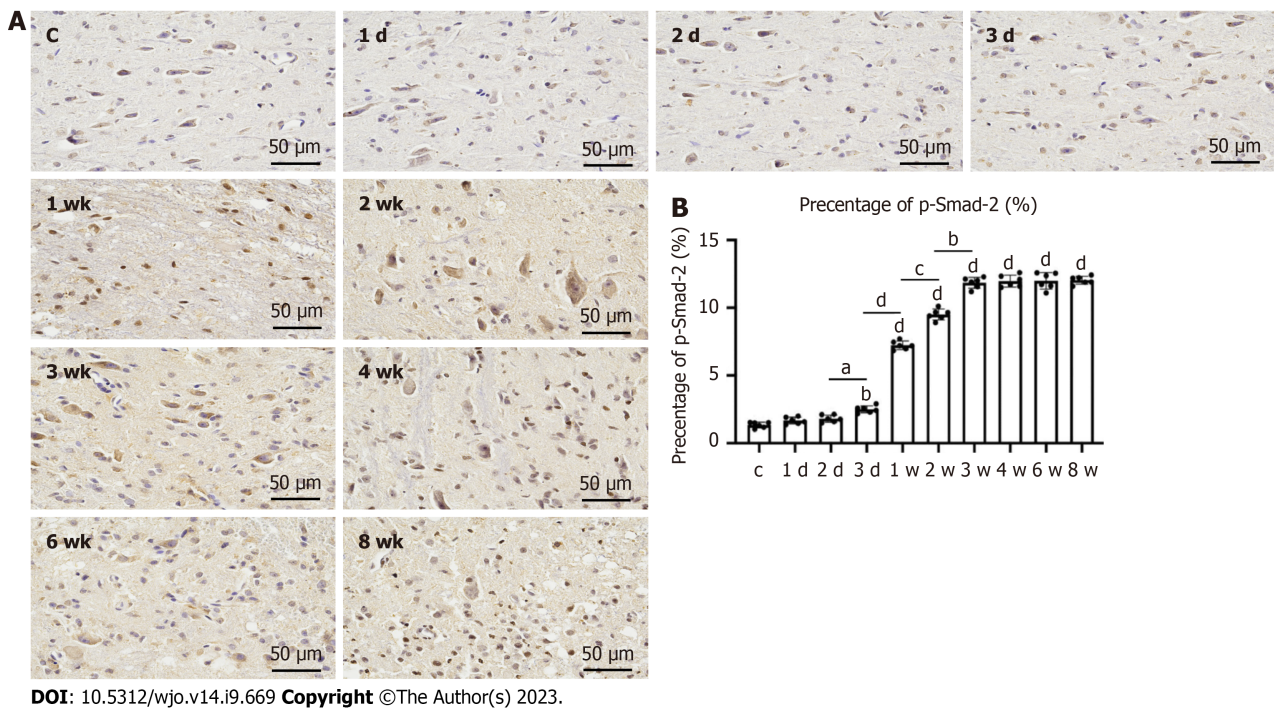


Figure 6 Immunohistochemistry findings. A: Immunohistochemical staining of the anterior joint capsule; B: Percentage of the anterior articular joint capsule phosphorylated mothers against decapentaplegic homolog 2. ^a $P < 0.05$; ^b $P < 0.01$; ^c $P < 0.001$; ^d $P < 0.0001$.

change, but there were significant differences only between the groups of immobilization-3 d and -1 wk, immobilization-1 wk and -2 wk ($P < 0.05$). In all of the results, with the exception of the fixed-1 d and -2 d groups, there was also a significant difference between the control group and the fixed group ($P < 0.05$) (Figure 7).

DISCUSSION

Joint contracture is a relatively common condition that is mainly caused by fibrosis of the joint capsule and skeletal muscle after long-term immobilization, and shows the pathological features of excessive deposition of collagen and connective tissue components[15]. Numerous animal models have been developed to simulate knee flexion contracture; however, few animal models of knee extension contracture have been reported. A previous study successfully established a model of knee extension contracture in New Zealand white rabbits and reported in detail the characteristics of plaster immobilization and the relevant mechanisms[16]. However, it is beneficial to model knee extension contracture in rats rather than rabbits because of the lower cost of studying the pathogenesis of joint contracture and evaluating therapeutic efficacy. Therefore, the present study described a method to establish a model of knee extension contracture in the rat. We demonstrated that this model had significantly limited knee flexion motion and altered expressions of histological and fibrosis-related proteins in the skeletal muscle and anterior joint capsule.

Wang *et al*[17] directly assessed the muscle limitations of rats with immobilized ankle joints and found that the initial flexion contracture of the knee is mainly due to muscle structures and is reversible and can spontaneously resolve. By contrast, long-term contracture is mainly caused by the joint structures and is irreversible[14]. Such arthrogenic contracture cannot be improved, even by aggressive rehabilitation[18]. Several reports suggest that joint contractures occur within 1 wk of immobilization and progress in a time-dependent manner[19,20]. Chimoto *et al*[21] reported that 2 wk of muscle limitation mainly causes myogenic contracture, while long-term contracture (more than 4 wk of immobilization) results in joint contracture. Therefore, prolonged immobilization for longer than 4 wk should be avoided to prevent irreversible joint contracture[22]. In the present study, myogenic contracture was the predominant type of contracture during the first 2 wk of immobilization. From 2 to 3 wk of immobilization, the joint contracture changed from myogenic to arthrogenic. The contracture initiation time in the present study was consistent with previous studies; however, in contrast with previous studies, the arthrogenic contracture stabilized at 3 wk and completely stable at 4 wk. Arthrogenic contracture is primarily a fibrotic response within the joint capsule. The posterior joint capsule is the main contributor to the formation of immobilization-induced knee flexion contracture, while the anterior joint capsule has the greatest impact on knee extension contracture[21]. The synovial layer of the anterior joint capsule is the widest and most complex in the knee joint[23]. In the present study, the degree of synovial hyperplasia continuously increased with the immobilization time; this may explain why knee extension contracture forms earlier than knee flexion contracture.

In the histologic assessment of the present study, the myofiber cross-sectional area, intermuscular collagen deposition, and extent of hyperplasia in the anterior joint capsule supported the biological findings. As the decreased skeletal muscle mass caused by an imbalance in protein metabolism is characterized by a significantly smaller muscle fiber area[24-26].

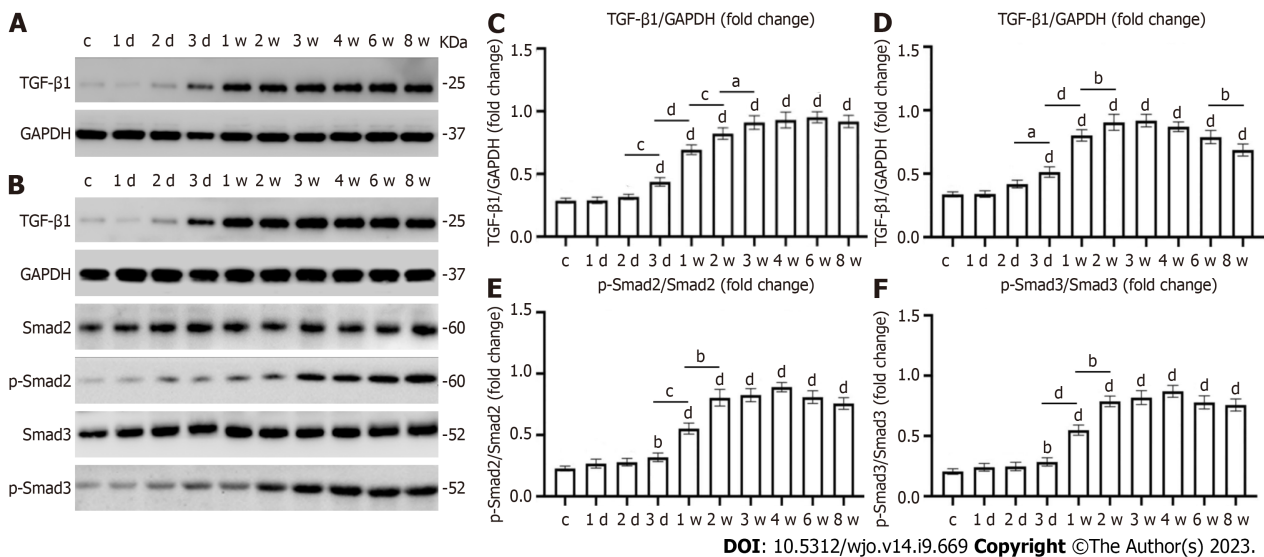


Figure 7 Western blot findings. A: Changes in the intensity of transforming growth factor beta 1 (TGF-β1) and glyceraldehyde 3-phosphate dehydrogenase (GAPDH) bands in the anterior joint capsule; B: Changes in the intensity of TGF-β1/GAPDH, phosphorylated mothers against decapentaplegic homolog 2 (p-Smad2)/Smad2, p-Smad2/Smad2 bands in the quadriceps; C: Graphical representation of the expression level of TGF-β1 in the anterior joint capsule relative to GAPDH; D-F: Graphical representation of the expression level of TGF-β1/GAPDH, p-Smad2/Smad2, p-Smad2/Smad2. ^aP < 0.05; ^bP < 0.01; ^cP < 0.001; ^dP < 0.0001.

The amount of intermuscular collagen deposition was significantly greater in the immobilization-1w group than the control group, but did not significantly differ between the immobilization-2 wk and -3 wk groups. Furthermore, there was significantly less intermuscular collagen deposition in the immobilization-6w group compared with the immobilization-4w group. This indicates that intermuscular collagen deposition began to increase in the 1st week of immobilization, but decreased after 4 wk of immobilization. Previous studies have shown that this may be associated with gradual resolution of the inflammatory and fibrotic response after immobilization[11]. This was demonstrated by the reduction in collagen content and TGF-β1 protein expression over time. The anterior joint synovial proliferation was significantly greater in the immobilization-2 d group than the control group, but did not differ between the immobilization-3 wk and -4 wk groups, indicating that the anterior joint synovial proliferation significantly increased during the first 3 wk of immobilization and completely stabilized from 4 wk onwards. Wang *et al*[27] analyzed changes in the synovial membrane caused by anterior articular capsule fibroblasts, microvasodilation, and congestion due to plaster immobilization. Li *et al*[28] and Yao *et al*[29] reported that intra-articular tissue adhesion does not completely cover the cruciate ligament in and around the knee, but originates from synovial fibrosis. The proliferation of intra-articular synovial tissue was responsible for the limited ROM found in the present study.

To further characterize the altered fibrosis of skeletal muscle and the joint capsule, we evaluated the expression of the TGF-β1 and p-Smad protein. There are three subtypes of TGF-β family: TGF-β1, TGF-β2, and TGF-β3. A large number of studies have demonstrated that the expression of TGF-β1 is the most important in fibrosis changes. TGF-β1 can cause differentiation, proliferation and extracellular matrix production, promote the transformation of fibroblasts to myofibroblasts, cause the deposition of collagen and increase the expression of alpha smooth muscle actin (α-SMA), and then cause tissue fibrosis[30,31]. Zhang *et al*[32] found that the expression level of TGF-β1 in the posterior joint capsule was significantly increased *in vivo* experiments. *In vitro* experiments showed that the expression level of TGF-β1 was increased, and the expression of α-SMA and type I collagen was also increased. Mao *et al*[33] applied a TGF-β inhibitor to treat a traumatic rat knee joint contracture animal model and found that after the activity of TGF-β was inhibited, the degree of joint contracture was alleviated, while the protein expression of collagen type I, collagen type III, α-SMA, and p-Smad2 was decreased. Therefore, we used the TGF-β1 and Smad signaling pathway as indicators to prove the formation of contracture. The aggravation of contracture enhances the fibrosis response, characterized by increases in profibrotic genes and proteins (*e.g.*, cytokine TGF-β1 genes, type I and type III collagen genes and proteins), leading to increases in collagen density and joint capsule thickness[34]. Hildebrand *et al*[35] reported the increased expression of type I and III collagen, TGF-β1, p-Smad2, and p-Smad3 in a rabbit post-traumatic flexion contracture model compared with control joint cysts. The increased mRNA levels of TGF-β1 may be related to collagen deposition inside and outside the articular capsule. Joint capsule fibrosis may be associated with the development of joint contracture. Similarly, the present study showed that the expression of fibrosis-related genes increased with prolonged immobilization, but the expression of TGF-β1, p-Smad2, and p-Smad3 in the rectus femoris decreased slightly after 3 wk of immobilization and was significantly decreased at 8 wk. The altered expression levels of TGF-β1 may be due to hypoxia or a reduction in collagen turnover or degradation rates[36]. Among several other roles, one of the adaptive responses of hypoxic cells is the upregulation of hypoxia-inducible factor 1 alpha (HIF-1α). The expression of TGF-β1 and HIF-1α is significantly upregulated during the transformation of fibroblasts to myofibroblasts, leading to the promotion of vascular endothelial growth factor (VEGF) gene expression[37]. The HIF-1α signaling pathway in turn regulates angiogenesis by inducing VEGF expression, thereby improving circulation and reducing the inflammatory response[38].

In the present study, ordinary gypsum and polymer gypsum were initially used to establish the extended knee contracture model. However, the rats inevitably gnawed the gypsum and there was also gypsum slippage. In the process of switching to an aluminum splint, we found that the knee joints of the rats could not be wrapped when fixed because the proximal lower limbs were short and strong. The present shape of the external immobilization device was determined after multiple improvements. The immobilization device comprised of aluminum plate pressurized at the distal end on the back of the foot that was plantarflexed at 60°. After the first proximal rectangular aluminum plate was used to fix the knee joint, the second inverted trapezoidal aluminum plate was wrapped around the knee to ensure that the knee was completely immobilized. Although this immobilization method is simple, the pressure strength must be carefully controlled. A pressure that is too high will easily cause poor limb circulation in rats. As aluminum is easy to shape, we were able to adjust the tightness of the external immobilization to resolve any swelling. Tokuda *et al*[39] successfully created a model of flexion contracture outside the knee joint; however, the external immobilization device used in the present study had less effect on the overall activity of the rats and better reflected the clinical situation in which the knee joint is usually fixed in extension after injury, leading to limited knee flexion after long-term immobilization. Therefore, to more closely mimic the clinical situation, we chose to create a model of knee extension contracture.

We demonstrated that the present model is as reliable as other animal models in reproducing the features of human joint contracture, including limited joint mobility, changes in the joint and muscle histology, and changes in the expression of fibrosis-associated proteins in the joint capsule *vs* muscle. The advantage of the present model is that it is easy to replicate because it does not require complex surgical procedures, the tools are easy to use, and the rat anesthesia and immobilization can be performed in a very short period of time. We described the detailed process of establishing a rat model of knee extension contracture, with photographs. The model closely replicates joint contracture caused by complications of immobilization, enabling researchers to investigate the etiology of joint contracture and establish new treatments. This model is a reliable tool, as described earlier. Contractures caused by long-term fixation are mainly caused by joint structure and are irreversible. Moreover, the mechanism by which movement after fixation may exacerbate joint contracture has not been fully explored[40]. As the external fixator is easy to shape and can be removed at any time. Therefore, this model can be used to study the prevention and treatment of knee extension contracture in rats, at the same time, it is possible to change the dressing and keep the wound dry during the fixation of traumatic knee joint contracture.

The present study had some limitations. First, in this model, the ankle joint and the knee joint were inevitably fixed together. Because the lower limb of the rat is shaped like a cone, the ankle joint was plantarflexed at 60° and fixed with the knee joint to prevent slippage of the aluminum splint. Second, the longest immobilization time in the present study was 8 wk. We plan to explore the continuous longer-term changes in fibrosis-related proteins in a future study. Finally, the state of the extension contracture after the removal of the external fixator was also studied and will be reported.

CONCLUSION

The results in this study suggest that the myogenic contracture is stabilized after 2 wk, whereas the arthrogenic contracture is stabilized after 3 wk and completely stable in 4 wk.

ARTICLE HIGHLIGHTS

Research background

There is currently no research on establishing a model of knee joint extension contracture in rats.

Research motivation

The extension contracture model is of clinical relevance because it better mimics fracture and bed-associated immobilization than the flexion contracture model.

Research objectives

Clarify the formation process of knee joint extension contracture in rats.

Research methods

Verify the formation process of extension contracture by observing pathology, detecting fibrotic proteins, and measuring joint range of motion.

Research results

All results show that the myogenic contracture tends to stabilize after 2 wk, and the arthrogenic contracture tends to stabilize after 3 wk and completely stable in 4 wk.

Research conclusions

The extension contracture model is of clinical relevance because it better mimics fracture and bed-associated immobilization than the flexion contracture model.

Research perspectives

This rat model may be a useful tool for studying the etiology of joint contracture and establishing new treatment methods.

ACKNOWLEDGEMENTS

We thank Professor Hua Wang from School of Public Health, Anhui Medical University for his valuable corrections and advice. Hua Wang participated in the guidance of experimental design: (1) Key Laboratory of Environmental Toxicology of Anhui Higher Education Institutes, Hefei 230032, China; and (2) Department of Toxicology, School of Public Health, Anhui Medical University, Hefei 230032, China.

FOOTNOTES

Author contributions: Zhou CX conceived the study, participated in its design and coordination, and drafted the manuscript; Wang F participated in the design of the study and performed the statistical analyses; Zhou Y participated in its design and coordination, and helped to draft the manuscript; Fang QZ drew the pictures in the manuscript; Zhang QB performed the statistical analysis in the revised manuscript; All authors read and approved the final manuscript.

Supported by Anhui Key Research and Development Program-Population Health, No. 201904a07020067; Anhui Provincial Health Research Project, No. AHWJ2022b063; Clinical Medicine Discipline Construction Project of Anhui Medical University in 2022 (Clinic and Preliminary Co-Construction Discipline Project), No. 2022 lcxkEFY010; 2022 National Natural Science Foundation Incubation Plan, No. 2022GMFY05; Clinical Medicine Discipline Construction Project of Anhui Medical University in 2022 (High-Level Personnel Training Program), No. 2022 lcxkEFY04 and No. 2022 lcxkEFY05.

Institutional animal care and use committee statement: All animal experiments conformed to the internationally accepted principles for the care and use of laboratory animals (Anhui Medical University; protocol no. LLSC20221126, Experimental Animal Ethics Committee of Anhui Medical University, Anhui, China).

Conflict-of-interest statement: The authors have no conflicts of interest to declare.

Data sharing statement: No additional data are available.

ARRIVE guidelines statement: The authors have read the ARRIVE guidelines, and the manuscript was prepared and revised according to the ARRIVE guidelines.

Open-Access: This article is an open-access article that was selected by an in-house editor and fully peer-reviewed by external reviewers. It is distributed in accordance with the Creative Commons Attribution NonCommercial (CC BY-NC 4.0) license, which permits others to distribute, remix, adapt, build upon this work non-commercially, and license their derivative works on different terms, provided the original work is properly cited and the use is non-commercial. See: <https://creativecommons.org/licenses/by-nc/4.0/>

Country/Territory of origin: China

ORCID number: Chen-Xu Zhou 0000-0002-1808-7947; Feng Wang 0000-0003-4548-2309; Yun Zhou 0000-0001-9011-9459; Qiao-Zhou Fang 0009-0001-4870-132X; Quan-Bing Zhang 0000-0003-2858-7723.

S-Editor: Qu XL

L-Editor: Filipodia

P-Editor: Xu ZH

REFERENCES

- 1 Sato Y, Ono T, Ishikura H, Aihara K, Tasaka A, Umei N, Tsumiyama W, Oki S. The recovery time required for rat joint contractures treated with joint fixation with unweighting of the hind limbs. *J Phys Ther Sci* 2019; **31**: 336-339 [PMID: 31037005 DOI: 10.1589/jpts.31.336]
- 2 Hinz B, Lagares D. Evasion of apoptosis by myofibroblasts: a hallmark of fibrotic diseases. *Nat Rev Rheumatol* 2020; **16**: 11-31 [PMID: 31792399 DOI: 10.1038/s41584-019-0324-5]
- 3 Winston BA, Jones J, Ries MD. Flexion contracture due to cyclops lesion after bicruciate-retaining total knee arthroplasty. *Arthroplast Today* 2019; **5**: 442-445 [PMID: 31886387 DOI: 10.1016/j.artd.2019.09.003]
- 4 Zhang QB, Zhou Y, Zhong HZ, Liu Y. Effect of Stretching Combined With Ultrashort Wave Diathermy on Joint Function and Its Possible Mechanism in a Rabbit Knee Contracture Model. *Am J Phys Med Rehabil* 2018; **97**: 357-363 [PMID: 29210704 DOI: 10.1097/PHM.0000000000000873]
- 5 Zhuang Z, Yu D, Chen Z, Liu D, Yuan G, Yirong N, Sun L, Liu Y, He R, Wang K. Curcumin Inhibits Joint Contracture through PTEN Demethylation and Targeting PI3K/Akt/mTOR Pathway in Myofibroblasts from Human Joint Capsule. *Evid Based Complement Alternat Med*

- 2019; **2019**: 4301238 [PMID: 31511778 DOI: 10.1155/2019/4301238]
- 6 **Yu D**, Zhuang Z, Ren J, Hu X, Wang Z, Zhang J, Luo Y, Wang K, He R, Wang Y. Hyaluronic acid-curcumin conjugate suppresses the fibrotic functions of myofibroblasts from contractive joint by the PTGER2 demethylation. *Regen Biomater* 2019; **6**: 269-277 [PMID: 31616564 DOI: 10.1093/rb/rbz016]
 - 7 **Wang F**, Zhang QB, Zhou Y, Chen S, Huang PP, Liu Y, Xu YH. The mechanisms and treatments of muscular pathological changes in immobilization-induced joint contracture: A literature review. *Chin J Traumatol* 2019; **22**: 93-98 [PMID: 30928194 DOI: 10.1016/j.cjtee.2019.02.001]
 - 8 **Akai M**, Shirasaki Y, Tateishi T. Viscoelastic properties of stiff joints: a new approach in analyzing joint contracture. *Biomed Mater Eng* 1993; **3**: 67-73 [PMID: 8369728]
 - 9 **Onda A**, Kono H, Jiao Q, Akimoto T, Miyamoto T, Sawada Y, Suzuki K, Kusakari Y, Minamisawa S, Fukubayashi T. New mouse model of skeletal muscle atrophy using spiral wire immobilization. *Muscle Nerve* 2016; **54**: 788-791 [PMID: 27227343 DOI: 10.1002/mus.25202]
 - 10 **Aihara M**, Hirose N, Katsuta W, Saito F, Maruyama H, Hagiwara H. A new model of skeletal muscle atrophy induced by immobilization using a hook-and-loop fastener in mice. *J Phys Ther Sci* 2017; **29**: 1779-1783 [PMID: 29184288 DOI: 10.1589/jpts.29.1779]
 - 11 **Kaneguchi A**, Ozawa J, Minamimoto K, Yamaoka K. Formation process of joint contracture after anterior cruciate ligament reconstruction in rats. *J Orthop Res* 2021; **39**: 1082-1092 [PMID: 32667709 DOI: 10.1002/jor.24800]
 - 12 **Trudel G**, Uthoff HK. Contractures secondary to immobility: is the restriction articular or muscular? An experimental longitudinal study in the rat knee. *Arch Phys Med Rehabil* 2000; **81**: 6-13 [PMID: 10638868 DOI: 10.1016/s0003-9993(00)90213-2]
 - 13 **Moriyama H**, Yoshimura O, Sunahori H, Tobimatsu Y. Comparison of muscular and articular factors in the progression of contractures after spinal cord injury in rats. *Spinal Cord* 2006; **44**: 174-181 [PMID: 16130021 DOI: 10.1038/sj.sc.3101802]
 - 14 **Trudel G**, Laneuville O, Coletta E, Goudreau L, Uthoff HK. Quantitative and temporal differential recovery of articular and muscular limitations of knee joint contractures; results in a rat model. *J Appl Physiol (1985)* 2014; **117**: 730-737 [PMID: 25123199 DOI: 10.1152/jappphysiol.00409.2014]
 - 15 **Le Sant G**, Nordez A, Andrade R, Hug F, Freitas S, Gross R. Stiffness mapping of lower leg muscles during passive dorsiflexion. *J Anat* 2017; **230**: 639-650 [PMID: 28251615 DOI: 10.1111/joa.12589]
 - 16 **Zhou Y**, Zhang QB, Zhong HZ, Liu Y, Li J, Lv H, Jing JH. Rabbit Model of Extending Knee Joint Contracture: Progression of Joint Motion Restriction and Subsequent Joint Capsule Changes after Immobilization. *J Knee Surg* 2020; **33**: 15-21 [PMID: 30562834 DOI: 10.1055/s-0038-1676502]
 - 17 **Wang F**, Zhou CX, Zheng Z, Li DJ, Li W, Zhou Y. Metformin reduces myogenic contracture and myofibrosis induced by rat knee joint immobilization via AMPK-mediated inhibition of TGF- β 1/Smad signaling pathway. *Connect Tissue Res* 2023; **64**: 26-39 [PMID: 35723580 DOI: 10.1080/03008207.2022.2088365]
 - 18 **Xu QY**, Zhang QB, Zhou Y, Liu AY, Wang F. Preventive effect and possible mechanisms of ultrashort wave diathermy on myogenic contracture in a rabbit model. *Sci Prog* 2021; **104**: 368504211054992 [PMID: 34825614 DOI: 10.1177/00368504211054992]
 - 19 **Nagai M**, Aoyama T, Ito A, Iijima H, Yamaguchi S, Tajino J, Zhang X, Akiyama H, Kuroki H. Contributions of biarticular myogenic components to the limitation of the range of motion after immobilization of rat knee joint. *BMC Musculoskelet Disord* 2014; **15**: 224 [PMID: 25001065 DOI: 10.1186/1471-2474-15-224]
 - 20 **Trudel G**, Uthoff HK, Goudreau L, Laneuville O. Quantitative analysis of the reversibility of knee flexion contractures with time: an experimental study using the rat model. *BMC Musculoskelet Disord* 2014; **15**: 338 [PMID: 25294116 DOI: 10.1186/1471-2474-15-338]
 - 21 **Chimoto E**, Hagiwara Y, Ando A, Itoi E. Progression of an arthrogenic motion restriction after immobilization in a rat experimental knee model. *Ups J Med Sci* 2007; **112**: 347-355 [PMID: 18484076 DOI: 10.3109/2000-1967-207]
 - 22 **Kaneguchi A**, Ozawa J, Kawamata S, Yamaoka K. Development of arthrogenic joint contracture as a result of pathological changes in remobilized rat knees. *J Orthop Res* 2017; **35**: 1414-1423 [PMID: 27601089 DOI: 10.1002/jor.23419]
 - 23 **Zhao X**, Meng F, Hu S, Yang Z, Huang H, Pang R, Wen X, Kang Y, Zhang Z. The Synovium Attenuates Cartilage Degeneration in KOA through Activation of the Smad2/3-Runx1 Cascade and Chondrogenesis-related miRNAs. *Mol Ther Nucleic Acids* 2020; **22**: 832-845 [PMID: 33230479 DOI: 10.1016/j.omtn.2020.10.004]
 - 24 **Wang F**, Zhang QB, Zhou Y, Liu AY, Huang PP, Liu Y. Effect of ultrashort wave treatment on joint dysfunction and muscle atrophy in a rabbit model of extending knee joint contracture: Enhanced expression of myogenic differentiation. *Knee* 2020; **27**: 795-802 [PMID: 32201041 DOI: 10.1016/j.knee.2020.02.013]
 - 25 **Jin SB**, Tian ZB, Ding XL, Guo YJ, Mao T, Yu YN, Wang KX, Jing X. The Impact of Preoperative Sarcopenia on Survival Prognosis in Patients Receiving Neoadjuvant Therapy for Esophageal Cancer: A Systematic Review and Meta-Analysis. *Front Oncol* 2021; **11**: 619592 [PMID: 34249675 DOI: 10.3389/fonc.2021.619592]
 - 26 **Wang F**, Li W, Zhou Y, Huang PP, Zhang QB. Radial extracorporeal shock wave reduces myogenic contracture and muscle atrophy via inhibiting NF- κ B/HIF-1 α signaling pathway in rabbit. *Connect Tissue Res* 2022; **63**: 298-307 [PMID: 34014138 DOI: 10.1080/03008207.2021.1920934]
 - 27 **Wang M**, Liu C, Xiao W. Intra-articular injection of hyaluronic acid for the reduction in joint adhesion formation in a rabbit model of knee injury. *Knee Surg Sports Traumatol Arthrosc* 2014; **22**: 1536-1540 [PMID: 23740323 DOI: 10.1007/s00167-013-2547-3]
 - 28 **Li X**, Chen H, Sun Y, Dai J, Wang S, Wang J, Yan L. Hydroxycamptothecin prevents intraarticular scar adhesion by activating the PERK signal pathway. *Eur J Pharmacol* 2017; **810**: 36-43 [PMID: 28603046 DOI: 10.1016/j.ejphar.2017.06.006]
 - 29 **Yao Z**, Wang W, Ning J, Zhang X, Zheng W, Qian Y, Fan C. Hydroxycamptothecin Inhibits Peritendinous Adhesion via the Endoplasmic Reticulum Stress-Dependent Apoptosis. *Front Pharmacol* 2019; **10**: 967 [PMID: 31551777 DOI: 10.3389/fphar.2019.00967]
 - 30 **Kaneguchi A**, Ozawa J, Minamimoto K, Yamaoka K. Active exercise on immobilization-induced contractured rat knees develops arthrogenic joint contracture with pathological changes. *J Appl Physiol (1985)* 2018; **124**: 291-301 [PMID: 28982941 DOI: 10.1152/jappphysiol.00438.2017]
 - 31 **Rodeo SA**, Hannafin JA, Tom J, Warren RF, Wickiewicz TL. Immunolocalization of cytokines and their receptors in adhesive capsulitis of the shoulder. *J Orthop Res* 1997; **15**: 427-436 [PMID: 9246090 DOI: 10.1002/jor.1100150316]
 - 32 **Zhang Y**, Liu Z, Wang K, Lu S, Fan S, Xu L, Cai B. Macrophage migration inhibitory factor regulates joint capsule fibrosis by promoting TGF- β 1 production in fibroblasts. *Int J Biol Sci* 2021; **17**: 1837-1850 [PMID: 33994866 DOI: 10.7150/ijbs.57025]
 - 33 **Mao D**, Mi J, Pan X, Li F, Rui Y. Suppression of TGF-beta activity with remobilization attenuates immobilization-induced joint contracture in rats. *Injury* 2021; **52**: 434-442 [PMID: 33408055 DOI: 10.1016/j.injury.2020.12.029]
 - 34 **Kaneguchi A**, Ozawa J, Minamimoto K, Yamaoka K. Low-Level Laser Therapy Prevents Treadmill Exercise-Induced Progression of

- Arthrogenic Joint Contracture Via Attenuation of Inflammation and Fibrosis in Remobilized Rat Knees. *Inflammation* 2019; **42**: 857-873 [PMID: 30506108 DOI: 10.1007/s10753-018-0941-1]
- 35 **Hildebrand KA**, Zhang M, Germscheid NM, Wang C, Hart DA. Cellular, matrix, and growth factor components of the joint capsule are modified early in the process of posttraumatic contracture formation in a rabbit model. *Acta Orthop* 2008; **79**: 116-125 [PMID: 18283583 DOI: 10.1080/17453670710014860]
- 36 **Hagiwara Y**, Ando A, Onoda Y, Matsui H, Chimoto E, Suda H, Itoi E. Expression patterns of collagen types I and III in the capsule of a rat knee contracture model. *J Orthop Res* 2010; **28**: 315-321 [PMID: 19777487 DOI: 10.1002/jor.20997]
- 37 **Huang PP**, Zhang QB, Zhou Y, Liu AY, Wang F, Xu QY, Yang F. Effect of Radial Extracorporeal Shock Wave Combined With Ultrashort Wave Diathermy on Fibrosis and Contracture of Muscle. *Am J Phys Med Rehabil* 2021; **100**: 643-650 [PMID: 32969968 DOI: 10.1097/PHM.0000000000001599]
- 38 **Zimmermann SM**, Würgler-Hauri CC, Wanner GA, Simmen HP, Werner CM. Echinomycin in the prevention of heterotopic ossification - an experimental antibiotic agent shows promising results in a murine model. *Injury* 2013; **44**: 570-575 [PMID: 23398900 DOI: 10.1016/j.injury.2012.12.030]
- 39 **Tokuda K**, Yamanaka Y, Kosugi K, Nishimura H, Okada Y, Tsukamoto M, Tajima T, Suzuki H, Kawasaki M, Uchida S, Nakamura E, Wang KY, Sakai A. Development of a novel knee contracture mouse model by immobilization using external fixation. *Connect Tissue Res* 2022; **63**: 169-182 [PMID: 33602048 DOI: 10.1080/03008207.2021.1892088]
- 40 **Kaneguchi A**, Ozawa J. Inflammation and Fibrosis Induced by Joint Remobilization, and Relevance to Progression of Arthrogenic Joint Contracture: A Narrative Review. *Physiol Res* 2022; **71**: 447-488 [PMID: 35770468 DOI: 10.33549/physiolres.934876]



Published by **Baishideng Publishing Group Inc**
7041 Koll Center Parkway, Suite 160, Pleasanton, CA 94566, USA
Telephone: +1-925-3991568
E-mail: bpgoffice@wjgnet.com
Help Desk: <https://www.f6publishing.com/helpdesk>
<https://www.wjgnet.com>

